Journal of Sound and Vibration (1984) **96**(1), 69–82

MODEL FOR THE VIBRATION PRODUCED BY A SINGLE POINT DEFECT IN A ROLLING ELEMENT BEARING

P. D. McFADDEN† AND J. D. SMITH

Cambridge University Engineering Department, Cambridge CB2 1PZ, England

(*Received* 15 *April* 1983 *and in revised form* 16 *November* 1983)

A model is developed to describe the vibration produced by a single point defect on the inner race of a rolling element bearing under constant radial load. The model incorporates the effects of bearing geometry, shaft speed, bearing load distribution, transfer function and the exponential decay of vibration. A comparison of predicted and measured demodulated vibration spectra confirms the satisfactory performance of the model.

1. INTRODUCTION

When a defect in one surface of a rolling element bearing strikes another surface, it produces an impulse which may excite resonances in the bearing and in the machine. As the bearing rotates, these impulses will occur periodically with a frequency which is determined uniquely by the location of the defect, be it on the inner race, outer race, or one of the rolling elements.

The resonance excited by the impulses can be detected by a vibration transducer mounted on the machine near the bearing. By bandpass filtering the signal from the transducer to isolate one resonant frequency, it is possible to exclude most of the vibration generated by other parts of the machine, enabling the vibration from the bearing to be identified even in a complex machine such as a gearbox. After filtering, the signal is demodulated by an envelope detector and its frequency spectrum is derived. It is then possible to detect the presence of a defect in the bearing by the appearance of a spectral line at the impulse repetition frequency associated with a defect on the inner race, outer race, or one of the rolling elements.

This sequence of operations, illustrated in Figure 1, forms the basis of the high-frequency resonance technique, sometimes referred to as demodulated resonance analysis, or envelope power spectral density analysis. This technique has been evolving slowly for many years [1–15]. It has proved successful in simple bearing configurations incorporating an outer race defect, but produces a confusing spectrum with many additional spectral lines if applied to bearings with defects on the inner race or rolling elements. Further problems arise when the damage to the bearing becomes extensive, as the pattern of spectral lines changes with increasing damage.

In spite of the long history of the high-frequency resonance technique, no model has been proposed which can explain satisfactorily the pattern of spectral lines observed and the manner in which these lines are influenced by the bearing parameters. Clearly, if the full potential of the high-frequency resonance technique is to be realized, an explanation for the appearance of the envelope spectrum must be developed. It is the purpose of this paper to provide such an explanation.

† Present address: Aeronautical Research Laboratories, PO Box 4331, Melbourne 3001, Australia.

0022-460X/84/170069+14 $03.00/0

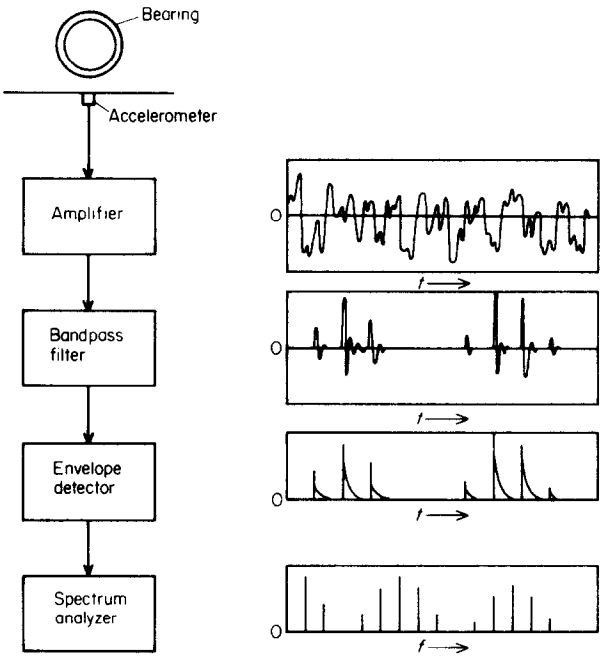

Figure 1. The operations involved in the high-frequency resonance technique and the form of the signals produced.

The generation of vibration by a point defect in a rolling element bearing will be modelled from first principles as a function of the rotation of the bearing, the distribution of load in the bearing, the transfer function between the bearing and the transducer, and the exponential decay of the resonances excited. In the course of the development, the effects of variations in these parameters will be discussed quantitatively and qualitatively. The derivation will be confined to the vibration generated by a single point defect on the inner race of a rolling element bearing under constant radial load. Extension of the model to include multiple point defects and outer race and rolling element defects under radial and axial load is required.

During development of the model, emphasis is placed on graphical presentation in both time and frequency domains in order to show clearly the effects of the load distribution, transfer function and decay of resonances on the envelope spectrum. Detailed mathematical descriptions of the functions are not attempted, simply because in practical applications of condition monitoring these functions are in general neither known nor of interest. It is hoped that this form of presentation will give a sound understanding of the principles involved, thereby making the extension of the model from single to multiple defects, and the search for improved methods of analysis, somewhat easier.

2. DEVELOPMENT OF MODEL

2.1. SINGLE INNER RACE DEFECT

The vibration produced by a single impact of a point defect with another bearing surface will be modelled as an impulse, represented by the impulse function $\delta(t)$ [16]. The severity of the defect will be represented by multiplying the impulse function by a constant d_0. The impulse represents the forcing function generated by the impact of the

defect, and as such forms the input to the bearing and the machine structure. The resonance which follows is the response of the bearing and the machine to that impulse, and will be considered in a later section.

As the bearing rotates, these impulses will occur periodically with a frequency which is dependent on the location of the defect. Equations are available which enable the frequency to be calculated from a knowledge of the bearing geometry and the shaft speed [9, 13]. Only inner race defects will be considered here, but the model can be applied to rolling element and outer race defects by suitable substitutions. For an inner race defect, impulses are generated when the defect strikes the rolling elements in the load zone as the shaft rotates. The frequency with which this impact occurs is known as the inner race element passing frequency, denoted here by f_d.

Before describing further the modelling of defects, it is necessary to select a reference point for specifying the angular position of the defect. In Figure 2, a rolling element bearing is shown with a radial applied load and an inner race defect, the position of which is specified by the angle θ between the defect and the line of application of the load. It will also be assumed that at time $t = 0$ the defect is located at the position $\theta = 0$, and is in contact with a rolling element.

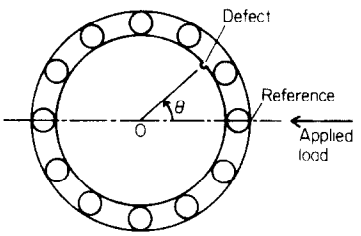

Figure 2. The angular position of a defect on the inner race relative to the reference position.

In the next section, the variations in load around the bearing will be examined, but for the present it is assumed that the impacts are produced by the rolling elements striking the defect under a unit load distributed uniformly around the bearing. Hence, the vibration produced by the defect can be modelled as an infinite series of impulses of equal amplitude, with the period between the impulses being T_d, the reciprocal of the inner race element passing frequency f_d. The function $d(t)$ is represented mathematically by the equation

$$d(t) = d_0 \sum_{k=-\infty}^{\infty} \delta(t - kT_d). \tag{1}$$

The function $d(t)$ is shown graphically in Figure 3(a) as a series of impulses of amplitude d_0 extending to infinity in both directions. Since it was assumed that at time $t = 0$ the defect and one rolling element were located at the position $\theta = 0$, then one impulse occurs at exactly $t = 0$.

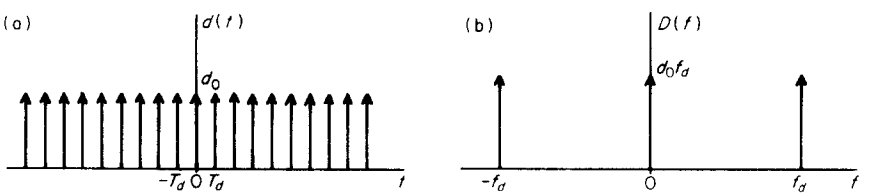

Figure 3. The impulses produced by an inner race defect under a unit load. (a) Time history; (b) spectrum.

The Fourier transform of an infinite series of impulses is also an infinite series of impulses. The transform of $d(t)$ is given by the equation [16]

$$D(f) = d_0 f_d \sum_{k=-\infty}^{\infty} \delta(f - kf_d). \tag{2}$$

This transform is shown graphically in Figure 3(b) as a series of impulses of amplitude $d_0 f_d$ extending to infinity in both directions, with a separation between the impulses equal to the inner race element passing frequency f_d.

The function $d(t)$ as defined here is both real and even, and therefore its Fourier transform $D(f)$ is also real and even [16]: that is, its imaginary part is zero for all f, and so the phase of $D(f)$ is zero for all f.

2.2. BEARING LOAD DISTRIBUTION

The distribution of the load around the circumference of a rolling element bearing under radial load is defined approximately by the Stribeck equation [17]

$$q(\theta) = q_0[1 - (1/2\varepsilon)(1 - \cos\theta)]^n, \tag{3}$$

where q_0 is the maximum load intensity, ε is the load distribution factor, θ_{max} is the angular extent of the load zone, and $n = 3/2$ for ball bearings and 10/9 for roller bearings. The terms q_0, ε and θ_{max} are all functions of the diametral clearance of the bearing and the applied load. For a bearing with positive clearance, $\varepsilon < 0{\cdot}5$ and $\theta_{max} < \pi/2$, giving a load distribution of the form shown in Figure 4. Note that for a part of each revolution

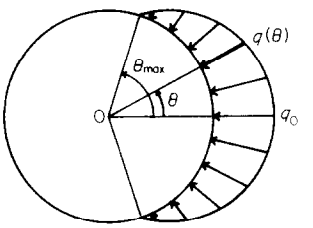

Figure 4. The load distribution in a bearing under a radial load.

the load applied to the rolling elements is zero. The actual clearance of the bearing is not important in the derivation of the model, and bearings with zero or negative clearance could be considered with equal ease.

The Stribeck equation shown above does not account for the changes in the load distribution which can occur due to the changing numbers and positions of the rolling elements in the load zone. However, from a detailed experimental study [18] it has been concluded that fluctuations in deflection and stiffness due to the changing numbers and positions of the elements can be less than 0·5% of the total value for a given load. These variations will be ignored in the development of the model.

If the inner race of the bearing is fitted to a shaft rotating at a constant frequency of f_s resolutions per second, then the instantaneous load on a point on the inner race as a function of time can be obtained by substituting $2\pi f_s t$ for θ in equation (3):

$$q(t) = \begin{cases} q_0[1 - (1/2\varepsilon)(1 - \cos\theta)]^n & \text{for } |\theta| < \theta_{max} \\ 0 & \text{elsewhere} \end{cases}. \tag{4}$$

Note that $q(t)$ is a periodic function, as a given point on the inner race of the bearing passes through the load zone with each revolution of the shaft. The function $q(t)$ is shown graphically in Figure 5(a) as a series of load distribution curves, extending to infinity in both directions. The separation between the centre of each load distribution curve is equal to the period T_s, the reciprocal of the shaft rotation frequency f_s. Since it was assumed in the last section that $\theta = 0$ at $t = 0$, then one load distribution curve is centred at $t = 0$.

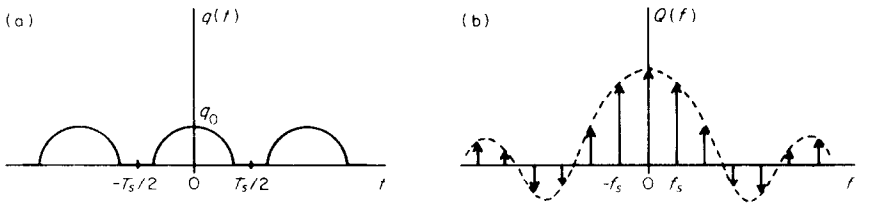

Figure 5. The load on the inner race of a bearing under a radial load. (a) Time history; (b) spectrum.

The approximate form of the Fourier transform of the function $q(t)$ is shown graphically in Figure 5(b). Because $q(t)$ is periodic in the time domain, its Fourier transform $Q(f)$ consists of a series of impulses in the frequency domain [16], separated by the shaft rotation frequency f_s. The envelope of the impulses is defined by the Fourier transform of the load distribution function for a single shaft revolution. If the load distribution factor $\varepsilon < 1{\cdot}0$, then discontinuities will exist at the beginning and the end of the load zone, causing the envelope of the Fourier transform to possess side lobes extending to infinity in both directions. In the case where $\varepsilon = 1{\cdot}0$, the load zone extends throughout the revolution of the shaft. No discontinuities exist, and so the Fourier transform is bounded in the frequency domain.

Increasing the shaft rotation frequency while maintaining the load distribution unchanged has the effect of contracting the time domain signal by scaling. In accordance with the time-scaling properties of the Fourier transform [16], the corresponding effect in the frequency domain is to expand the Fourier transform in frequency by the same factor and divide its amplitude by that factor. If the angular extent of the load zone is increased while the shaft frequency is held constant, then the main lobe and side lobes of the envelope in the frequency domain will be narrowed. The frequencies of the impulses will remain unchanged, but their amplitudes will vary as the envelope is narrowed.

The function $q(t)$ as defined here is both real and even and therefore its Fourier transform $Q(f)$ is also real and even [16]: that is, its imaginary part is zero for all f, and so the phase of $Q(f)$ is zero for all f.

2.3. MODULATION OF IMPULSES BY LOAD

In the preceding sections, equations were developed which describe firstly the series of impulses produced by a defect on the inner race of a rolling element bearing acting under a constant unit load, and secondly, the actual load distribution in a bearing with an applied radial load. These equations will now be combined to give an expression for the impulses produced in a bearing under radial load.

It is assumed initially that the amplitude of the impulse produced by a defect is directly proportional to the load on the rolling element when it strikes the defect. In this manner an expression for the amplitude of the impulses can be obtained by multiplying the series of impulses $d(t)$, produced under unit load, by the actual load distribution $q(t)$. The

formation of the product $d(t)q(t)$ is illustrated graphically in Figure 6(a). Note that the frequency of $d(t)$ is not necessarily an integer multiple of the frequency of $q(t)$, because the relationship between their frequencies is determined by the bearing geometry. Hence the pattern of impulses produced by the product $d(t)q(t)$ is different from one shaft revolution to the next.

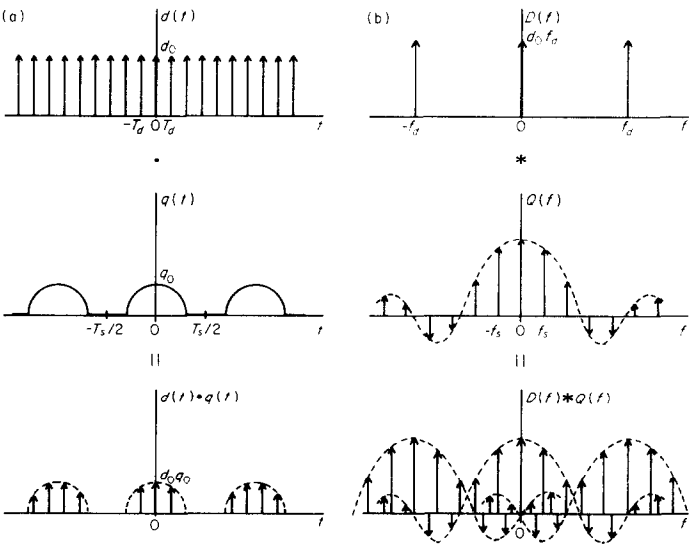

Figure 6. The impulses produced by an inner race defect under a radial load. (a) Time histories; (b) spectra.

According to the convolution theorem [16], if two signals are multiplied in the time domain, then their Fourier transforms are convolved in the frequency domain. The convolution of $D(f)$ and $Q(f)$ causes $Q(f)$ to be replicated in the frequency domain at intervals of f_d, extending to infinity in both directions, as shown in Figure 6(b). Depending upon the shape of the envelope of $Q(f)$ and the separation f_d, there may be extensive overlapping of the side lobes of one group with the main lobes and side lobes of adjoining groups.

Since the functions $d(t)$ and $q(t)$ as defined here are both real and even, their product $d(t)q(t)$ and its Fourier transform $D(f) * Q(f)$ are also real and even [16]: that is, the imaginary part and the phase of $D(f) * Q(f)$ are zero for all f.

2.4. TRANSMISSION OF VIBRATION

When an impulse is applied to the bearing, it will excite resonances in the bearing and the machine which can be measured by a vibration transducer at a nearby location on the casing of the machine. The vibration measured by the transducer is termed the impulse response of the mechanical system comprising the bearing and the machine. The Fourier transform of the impulse response gives the transfer function between the point at which the impulse was applied and the measurement location. It is likely that the actual response will include several resonances. However, in the high-frequency resonance technique it is usual to isolate one resonance by bandpass filtering of the transducer output. For simplicity, it will be assumed in the remaining discussion that only one resonance occurs.

Figure 7 shows a schematic diagram of the bearing, machine and transducer. It is assumed that the sensitive axis of the transducer lies on the reference line through $\theta = 0$,

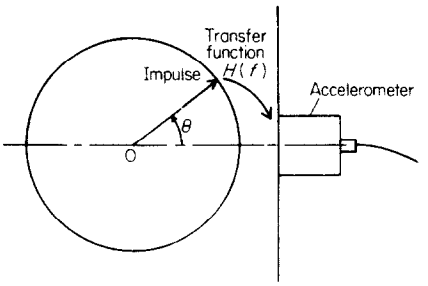

Figure 7. The transmission of vibration from the bearing to the transducer.

and that the machine structure is symmetrical about this line. If a unit impulse is applied to the bearing at a location defined by the angle θ, the vibration measured by the transducer will be the unit impulse response function $h(t)$. It is assumed that $h(t)$ takes the form of an exponentially decaying sinusoid, as illustrated in Figure 8(a). The transfer function $H(f)$ between the location on the bearing and the transducer is shown in Figure 8(b).

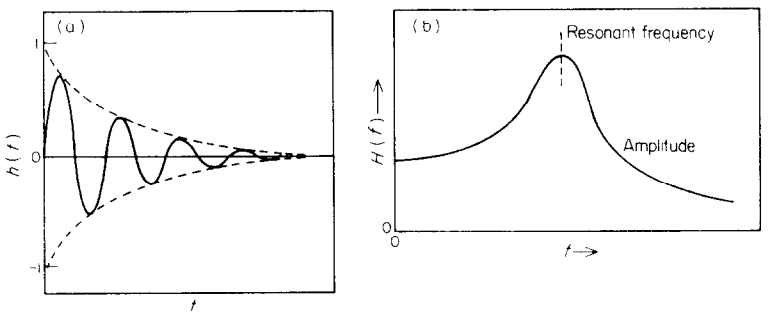

Figure 8. The impulse response and transfer function of the bearing and machine. (a) Time history; (b) spectrum.

For a linear system with a single degree of freedom, the vibration transmission characteristics can be specified at a given resonant frequency by the amplitude and phase of the response and the time constant of the exponential decay. As the angle θ changes, it is likely that the impulse response $h(t)$ and the transfer function $H(f)$ will also change due to the changing transmission path and angle of the applied impulse.

In the high-frequency resonance technique, the actual resonance is not of interest, but only the demodulated resonance, which permits an important simplification to be applied. It is assumed that the period of the demodulated signal, equal to the time between impacts of the defect with successive rolling elements, is much greater than the time required for an impulse to propagate from one side of the bearing to the other. Therefore the change in phase of the demodulated signal with changing angle θ will be negligible, except perhaps for very large bearings with many rolling elements operating at very high speeds. The transmission characteristics of the demodulated vibration can now be specified at a given resonant frequency by the amplitude of the response and the time constant of the decay.

If it is further assumed that the time constant of the exponential decay is independent of the angle θ, then the response measured at the transducer due to an impulse applied to the bearing at the location θ can be characterized simply by an amplitude which is a

function of θ. The impulse response function $h(t)$ and the transfer function $H(f)$ can be replaced by a function $a(\theta)$ giving the amplitude and sign of the transfer function $H(f)$ at each angle θ, and by the exponential decay of a unit impulse, denoted by the function $e(t)$. For a defect on the inner race of the bearing, rotating at a constant frequency of f_s revolutions per second, the instantaneous amplitude of the transfer function between the defect and the transducer as a function of time, denoted by $a(t)$, can be obtained by substituting $2\pi f_s t$ for θ.

Note that $a(t)$ is a periodic function, as the variations in the transfer function repeat with each revolution of the shaft. At $\theta = 0$, it is probable that $a(t)$ will have a maximum value as the impulse is applied close to the transducer and in the direction of the sensitive axis. When $\theta = \pi$, the magnitude of $a(t)$ will be less than at $\theta = 0$ because the distance to the transducer is greater. The sign of $a(t)$ may also be reversed because the impulse is applied in the opposite direction, but this will depend on the mode of the vibration at the resonant frequency examined. At $\theta = \pi/2$ and $3\pi/2$ the value of $a(t)$ may be near zero as the direction of the impulses will be perpendicular to the sensitive axis of the transducer, but this will also depend on the mode of the vibration. Behaviour of this type has been observed in practice [1].

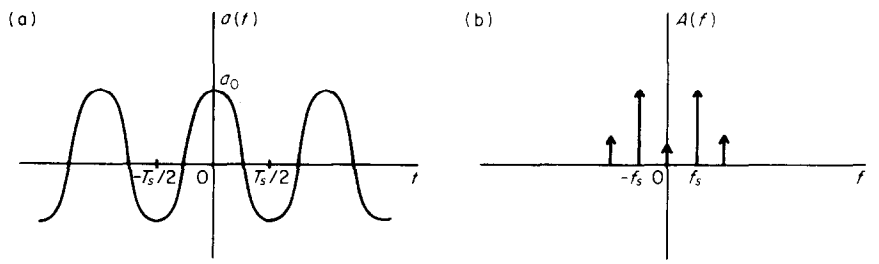

Figure 9. The variations in the amplitude of the transfer function. (a) Time history; (b) spectrum.

A possible form of the function $a(t)$ is shown in Figure 9(a) as a continuous, periodic curve, extending to infinity in both directions. The period of the function is equal to the period of the shaft rotation T_s. Since it was assumed that the transducer is situated at the reference position and that the machine structure is symmetrical about this position, then the function $a(t)$ is even.

The approximate form of the Fourier transform of $a(t)$ is shown graphically in Figure 9(b). Because $a(t)$ is periodic in the time domain, its Fourier transform $A(f)$ consists of a series of impulses in the frequency domain [16], separated by the shaft rotation frequency f_s. If the function $a(t)$ is continuous in the time domain, then $A(f)$ will be bounded in the frequency domain.

The function $a(t)$ as defined here is both real and even, and therefore its Fourier transform $A(f)$ is also real and even [16]: that is, its imaginary part is zero for all f, and so the phase of $A(f)$ is zero for all f.

2.5. AMPLITUDE OF VIBRATION

In the preceding sections, expressions were developed for the amplitude of the impulses produced at the location of the defect in a bearing under radial load, and for the amplitude of the transfer function between the location of the defect and a transducer on the machine casing. These expressions will now be combined to give an expression for the amplitude

of the demodulated response produced at the transducer by a defect in a bearing under radial load.

The amplitude of the response at the transducer is given by the product of the impulses produced in the bearing under radial load $d(t)q(t)$ with the amplitude of the transfer function $a(t)$. The formation of the product $d(t)q(t)a(t)$ is illustrated graphically in Figure 10(a). Note that the periods of functions $q(t)$ and $a(t)$ are both equal to T_v.

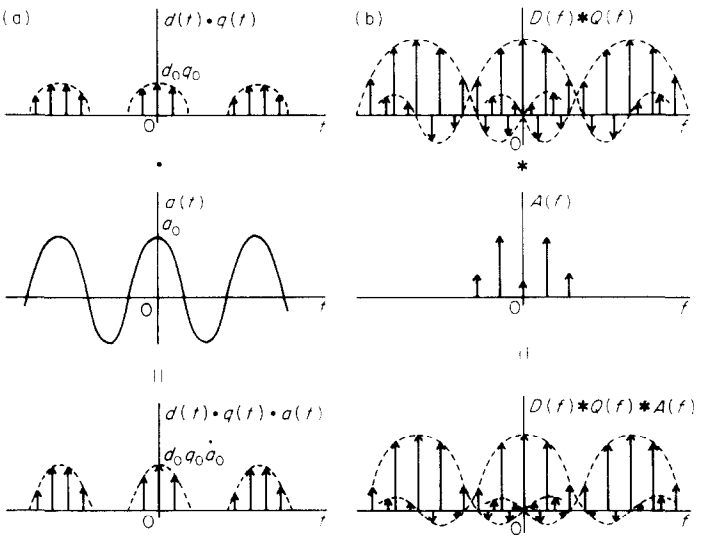

Figure 10. The impulses produced by an inner race defect under a radial load. (a) Time histories; (b) spectra.

According to the convolution theorem [16], if two or more signals are multiplied in the time domain, then their Fourier transforms are convolved in the frequency domain. The convolution of $D(f) * Q(f)$ and $A(f)$ causes the amplitudes of the components of $D(f) * Q(f)$ to be modified by convolution with the weighted impulses of the function $A(f)$, as shown in Figure 10(b). The frequencies of the components remain unchanged. Alternatively, the convolution $D(f) * Q(f) * A(f)$ can be viewed as the convolution of $D(f)$ with $Q(f) * A(f)$, in which case $Q(f) * A(f)$ is replicated in the frequency domain at intervals of f_d, extending to infinity in both directions. The result is identical.

Since the functions $d(t)$, $q(t)$ and $a(t)$ as defined here are both real and even, their product $d(t)q(t)a(t)$ and its Fourier transform $D(f) * Q(f) * A(f)$ are also real and even [16]: that is, the imaginary part and the phase of $D(f) * Q(f) * A(f)$ are zero for all f.

2.6. DECAY OF AN IMPULSE

In a preceding section it was shown that the demodulated vibration measured by a transducer on the casing of the machine due to a unit impulse applied to the bearing could be represented by the amplitude of the transfer function between the bearing and the transducer, and by the exponential decay of a unit impulse.

The decay of a unit impulse can be defined by the equation

$$e(t) = \begin{Bmatrix} e^{-t/T_e} & \text{for } t > 0 \\ 0 & \text{elsewhere} \end{Bmatrix}, \tag{5}$$

where T_e is the time constant of the decay. This function is shown graphically in Figure 11(a). The amplitude and phase of the Fourier transform of $e(t)$ are given by

$$|E(f)| = T_e/\sqrt{1+(2\pi f T_e)^2}, \qquad \arg[E(f)] = \arctan(-2\pi f T_e). \tag{6, 7}$$

These are shown graphically in Figure 11(b).

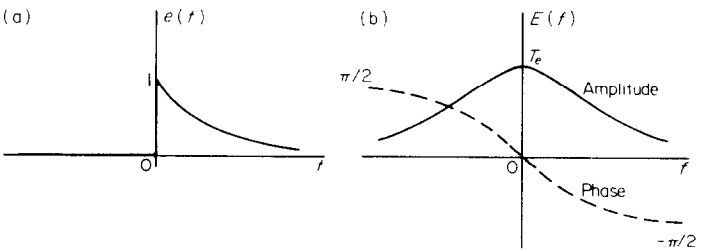

Figure 11. The exponential decay of an impulse. (a) Time history; (b) spectrum.

The function $e(t)$ is real, and therefore its Fourier transform $E(f)$ has a real part which is even and an imaginary part which is odd [16]; hence the amplitude of $E(f)$ is even but its phase is odd.

Note that increasing the time constant T_e causes the decay of the impulse to occur more slowly. The effect in the frequency domain of an increase in the time constant is to increase the amplitude at zero frequency, but to cause the roll-off of amplitude with increasing frequency to be more rapid. The net effect is to narrow the central maximum of the transform.

2.7. DECAY OF MODULATED IMPULSES

In the preceding sections, equations were developed which describe firstly the series of impulses produced by a defect on the inner race of a rolling element bearing acting under a radial load, and secondly the demodulated response of the bearing and machine to a unit impulse. These equations will now be combined to give an expression for the demodulated response of the bearing and machine to the impulses produced by the defect.

The demodulated response $v(t)$ is obtained by the convolution of the series of impulses produced by the defect with the response of the machine:

$$v(t) = [d(t)q(t)a(t)] * e(t). \tag{8}$$

This function is shown graphically in Figure 12(a).

According to the convolution theorem [16], if two signals are convolved in the time domain, then their Fourier transforms are multiplied in the frequency domain. Hence the Fourier transform of function $v(t)$ is given by

$$V(f) = [D(f) * Q(f) * A(f)]E(f). \tag{9}$$

This is shown graphically in Figure 12(b).

It can be seen that the amplitude of all the lobes now decreases with increasing frequency. As a consequence, the component at zero frequency has the greatest amplitude in the spectrum, unless cancellation is caused by a component from one of the overlapping side lobes. It is clear from equation (6) that, for large frequencies, the amplitude of the Fourier transform of the decay function is inversely proportional to frequency. Consequently, for large values of frequency, the envelope of the main lobes should approach a rate of roll-off of 6 dB per octave.

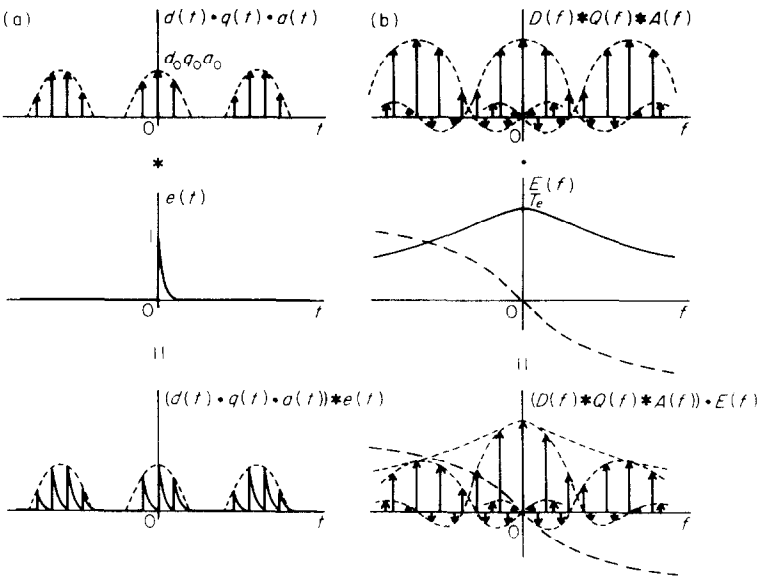

Figure 12. The impulses produced by an inner race defect under a radial load. (a) Time histories; (b) spectra.

It will also be noted that only the lobe which is centred at zero frequency is symmetrical about its centreline. Groups which are centred at other frequencies are no longer symmetrical, with the components on the low frequency side of their main lobe having a greater amplitude than the corresponding components on the high frequency side.

3. EXPERIMENTAL RESULTS

In this section, the predictions from the model for the bearing vibration are compared with experimental results. It will be shown that the frequencies and relative amplitudes of the lines in the predicted spectrum agree with those found in the measured spectrum.

Experiments were performed on a bearing test rig consisting of a shaft on which was fitted an RHP type 6209 C3 ball bearing. A single defect, approximately 0·5 mm wide, was etched with nitric acid on the inner race of the bearing, to simulate early spalling damage. The outer race of the bearing was pressed into a hole in the centre of a steel plate. The bearing was placed in pure radial load by a tensile force applied to one edge of the plate, while the vibration was measured by a high-frequency accelerometer mounted at the centre of the opposite edge of the plate. This arrangement is shown in Figure 13.

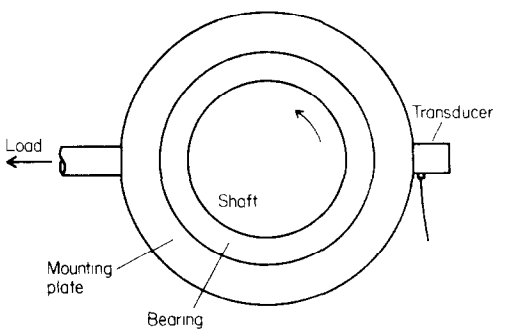

Figure 13. The bearing test rig.

Throughout the tests, the shaft was driven at a constant speed of 10 rev/s. From a knowledge of the bearing geometry, the nominal inner race element passing frequency at this shaft speed was calculated to be 53·8 Hz, although some variation will occur between bearings due to slight differences in geometry.

The measured vibration was processed by using the standard high-frequency resonance technique. The signal from the accelerometer was amplified by a charge amplifier, bandpass filtered to isolate a resonance in the frequency range 22–24 kHz, demodulated by using a half-wave rectifier and low-pass filter, and input to a minicomputer. Fourier transforms were calculated from blocks of 4096 samples in order to achieve adequate resolution of the many spectral lines. A minimum four-term Blackman–Harris weighting function [19, 20] was used to reduce the losses due to the picket-fence effect to less than 0·83 dB. It was not possible to determine the true amplitude of the component at zero frequency because of internal d.c. offsets in the equipment.

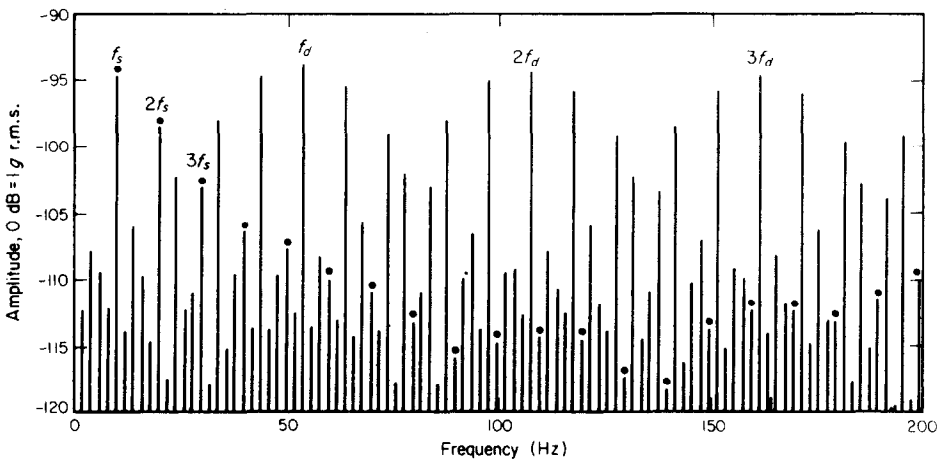

Figure 14. The envelope spectrum obtained from the test bearing with an inner race defect under a radial load.

The amplitude spectrum obtained for a load of 0·5 kN is shown in Figure 14. Examination of this spectrum shows that it contains a number of overlapping groups of spectral lines, centred at multiples of the inner race element passing frequency. Each group is composed of spectral lines separated by 10 Hz, the shaft rotation frequency. The form of each group is the same, consisting of a main lobe and side lobes. For the bearing tested, the inner race element passing frequency is such that the spectral lines from every fifth group coincide, at least within the resolution of the spectrum presented here. Comparison of the spectra in Figures 12(b) and 14 show that the structure of the spectrum predicted by the model is consistent with the structure of the measured spectrum, although the attenuation of the groups with increasing frequency has been exaggerated in Figure 12(b).

4. CONCLUSIONS

A model has been developed to describe the amplitude spectrum of the demodulated vibration produced by a rolling element bearing under constant radial load with a single point defect on its inner race. The vibration is modelled as the product of a series of impulses at the rolling element passing frequency with the bearing load distribution and

the amplitude of the transfer function, convolved with the impulse response of the exponential decay function.

The model is very simple, yet incorporates quantitatively the effects of bearing geometry, shaft speed, bearing load distribution, the transfer function between the bearing and the accelerometer, and the exponential decay of vibration. In its present form, the model is applicable only to a single point defect on the inner race of a bearing under radial load. Extension of the model to include multiple point defects and outer race and rolling element defects under radial and axial load is required.

A comparison of predicted and measured spectra for a bearing with an inner race defect and a radial load has shown that the model correctly predicts the frequencies and relative amplitudes of the components of the spectrum. It is hoped that this improved understanding will provide the first step in the development of improved methods of condition monitoring of rolling element bearings by vibration analysis.

ACKNOWLEDGMENTS

The authors wish to thank the staff of the Cambridge University Engineering Department and RHP for their assistance.

REFERENCES

1. J. J. BRODERICK, R. F. BURCHILL and H. L. CLARK 1972 *NASA CR* 123717. Design and fabrication of prototype system for early warning of impending bearing failure.
2. R. F. BURCHILL 1973 *Proceedings of 18th Meeting of Mechanical Failures Prevention Group, National Bureau of Standards NBSIR* 73-252, 21-29. Resonant structure techniques for bearing fault analysis.
3. R. F. BURCHILL, J. L. FRAREY and D. S. WILSON 1973 *Society of Automotive Engineers Paper* 730930. New machinery health diagnostic techniques using high-frequency vibration.
4. M. S. DARLOW, R. H. BADGLEY and G. W. HOGG 1974 *U.S. Army Air Mobility Research and Development Laboratory, USAAMRDL-TR-74-77*. Applications of high frequency resonance techniques for bearing diagnostics in helicopter gearboxes.
5. M. S. DARLOW and R. H. BADGLEY 1975 *Society of Automotive Engineers Paper* 750209. Early detection of defects in rolling-element bearings.
6. M. S. DARLOW and R. H. BADGLEY 1975 *American Society of Mechanical Engineers Paper 75-DET-46*. Applications for early detection of rolling element bearing failures using the high-frequency resonance technique.
7. D. B. BOARD 1975 *Proceedings of 10th Symposium on Non-Destructive Evaluation, San Antonio, Texas, 23-25 April*, 8-18. Incipient failure detection in high-speed rotating machinery.
8. D. B. BOARD 1975 *American Society of Mechanical Engineers Paper 75-WA/DE-16*. Incipient failure detection in CH-47 helicopter transmissions.
9. O. L. SANDORA 1976 *U.S. Army Air Mobility Research and Development Laboratory, USAAMRDL-TR-76-36*. Transmission condition assessment.
10. D. R. HARTING 1977 *Instrumentation Technology* **24**(9), 59–63. Incipient failure detection by demodulated resonance analysis.
11. D. R. HARTING 1978 *ISA Transactions* **17**, 35–40. Demodulated resonance analysis—a powerful incipient failure detection technique.
12. R. G. HERBERT and P. GADD 1978 *The Detection and Diagnosis of Bearing Faults by Vibration Analysis*. Naval Aircraft Materials Laboratory, Gosport, Hampshire.
13. K. NISHIO, S. HOSHIYA, T. MIYACHI and M. MATSUKI 1979 *American Society of Mechanical Engineers Paper 79-DET-45*. An investigation of the early detection of defects in ball bearings by the vibration monitoring.
14. R. M. STEWART 1980 *Applications of Time Series Analysis, Institute of Sound and Vibration Research, University of Southampton* 16.1–16.23. Application of signal processing techniques to machinery health monitoring.

15. A. G. RAY 1980 *2nd International Conference on Vibrations in Rotating Machinery, Institution of Mechanical Engineers, Cambridge*, 1–4 *September*, 187–194. Monitoring rolling contact bearings under adverse conditions.
16. E. O. BRIGHAM 1974 *The Fast Fourier Transform*. Englewood Cliffs, New Jersey: Prentice–Hall. See pp. 22, 32, 45, 58, 61, 224.
17. T. A. HARRIS 1966 *Rolling Bearing Analysis*. New York: John Wiley. See p. 148.
18. M. F. WHITE 1979 *Transactions of the American Society of Mechanical Engineers, Journal of Applied Mechanics* **46**, 677–684. Rolling element bearing vibration transfer characteristics: effect of stiffness.
19. F. J. HARRIS 1978 *Proceedings of the Institute of Electrical and Electronic Engineers* **66**, 51–83. On the use of windows for harmonic analysis with the discrete Fourier transform.
20. A. H. NUTTALL 1981 *Institute of Electrical and Electronic Engineers, Transactions on Acoustics, Speech, and Signal Processing* **ASSP-29**, 84–91. Some windows with very good sidelobe behaviour.